



Process optimization studies of malachite green dye adsorption onto areca husk carbon using response factorial design

A. Basker^{1*}, P. S. Syed Shabudeen², S. Daniel² and D. Kalaiselvi³

¹Department of Chemistry, Kalaignar Karunanidhi Institute of Technology, Coimbatore, Tamil Nadu (India)

²Department of Chemistry, Kumaraguru College of Technology, Coimbatore, Tamil Nadu (India)

³Department of Chemistry, Sri Shakthi Institute of Engineering and Technology, Coimbatore, Tamil Nadu (India)

ABSTRACT

In this study, a factorial experimental design technique was used to investigate the adsorption of malachite green (MG) from waste water onto Areca Husk Carbon (AHC). There is a growing interest in using low-cost and commercially available materials for the adsorption of dyes. The main and interaction effects of three different experimentally controlled environmental factors like pH, Particle Size and temperature are investigated through the model equations designed by a factorial design. The experimental factors and their respective levels that were selected include a pH of 4-9, particle size of 100-250 BSS mesh, and a temperature of 300-320 K. The results were analyzed statistically using the t-test, ANOVA, F-test and lack of fit to define most important process variables affecting the percentage MG removal.

Keywords: AHC, Crystal violet, Factorial design, ANOVA.

INTRODUCTION

Based on the quality of water with reference to the pollution, industries have been classified into three different categories namely orange, red and green. There are seventeen types of industries that have been classified as highly polluting, among which industries of dyes and chemicals are considered one. Since dyes are used in the textile manufacturing, it is imperative that the effluent generated from the textile industry needs to be treated and discharged if not recycled within the industry. The industries have been compelled to install reverse osmosis system, which have become mandatory recently. In view of this, it is quite essential that existing water bodies need to be protected from the effect of pollution. Though the concept of reuse, recycle and reduce have been very well conceived by the industries, efforts in that direction need to be accelerated.

In this context the present study of textile effluent treatment assumes great importance for developing low cost-effective waste water treatment technology as one of the best alternative ways to conserve water resources. Although there are various methods available to treat wastewater of textiles industries, there is a greater need for developing low cost-effective methods. Further, sludge generated from textile processing industries by conventional treatment technologies have proved inefficient. So far, there is no viable technology available to treat the sludge and it is just stored in the storage sheds. A suitable technology with zero generation of sludge will therefore help to contain the problem of sludge disposal. In this connection, it is to be stated that any treatment that reduces the quantity of sludge and recycle the wastewater after treatment will mitigate the problem of pollution and hazardous waste disposal. Such a study has not been taken up by earlier researchers, and, keeping this in view as a focal point. There are several

methods used for textile effluent treatment of dye containing wastewater. Some of them involve reverse osmosis [1], chemical oxidation [2], photo degradation [3], electrocoagulation[4] and adsorption[5].The present study is investigated to develop a low cost effective method of treatment of textile dye.

EXPERIMENTAL SECTION

Preparation of activated carbon adsorbent : One part by weight of each powdered raw material was chemically activated by treating with two parts by weight of concentrated sulphuric acid with constant stirring and was kept for 24 hours in a hot air oven at 75°C, the carbonized material was washed well with plenty of water several times to remove excess acid, surface adhered particles, water soluble materials dried at 200°C in hot air oven for 24 hours. Then it was taken in an iron vessel in muffle furnace and the temperature was gradually raised to 550°C for an hour, ground well by using ball mill and then sieved into particle size of 100,150 and 250 BSS Mesh size sand kept in air tight containers for further use.

Analysis of Malachite green

The concentration of MG in the supernatant solution before and after adsorption was determined using a double beam UV spectrophotometer (Shimadzu Japan) at a wavelength of 618 nm. It was found that the supernatant from the activated carbon did not exhibit any absorbance at this wavelength and also that the calibration curve was very reproducible and linear over the concentration range used in this work. The chemical structure of MG was shown in fig. 1.

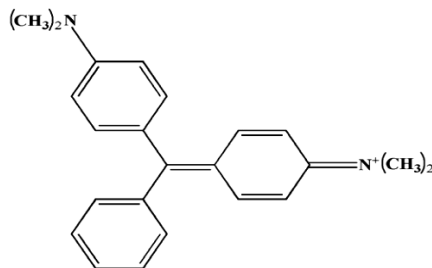


Fig.1. Chemical structure of Malachite Green

Batch equilibrium studies

Batch experiments were carried out by shaking 100 ml of dye solution (20 mg L⁻¹) with 150 mg of adsorbent in a glass stopper conical flask at a temperature at 30°C at the rate of 120 rpm. After agitation the solution centrifuged. Then the dye concentration in the supernatant solution was analyzed using a spectrophotometer by monitoring the absorbance changes at a wavelength of maximum absorbance (618nm) in these sorption experiments, the solution pH of 4-9.Each experiment was carried out and average results are presented. Calibration curves were obtained with standard MG solution using distilled water as a blank. Percent removal is calculated from the difference between the initial and final concentration of MG.

$$\% \text{ Removal} = \frac{(C_0 - C_e)}{C_0} \times 100 \quad (1)$$

Where C₀ and C_e (mg L⁻¹) are the liquid-phase concentrations of dye at initial and equilibrium respectively.

RESULTS AND DISCUSSION

SEM morphology

It is widely used to study the morphological features and surface characteristics of the adsorbent materials. Typical SEM photographs are shown in Fig. 2. It reveals that the AHC has a rough surface with more porous and caves like structure and it is supported with FTIR spectra as shown in Fig.3.

Determination of functional group

The FT-IR spectrum of AHC was detected in the range of 4000 to 400 cm⁻¹ was presented in Fig.3. The band observed at 3425.58cm⁻¹ was assigned to a ν(O-H) stretching vibration. The absorption band at 2854.65 and

2924.09 cm^{-1} can be attributed to the stretching vibrations of $\nu(\text{C-H})$ bonds in alkane and alkyl groups where carbon is bonded with hydrogen bonds. Adsorption bands at 2337.72 and 2376.30 cm^{-1} corresponds to $\nu(\text{N-H})$ stretching. The band at 1573.91 cm^{-1} shows the asymmetric $\nu(\text{-COO-})$ stretching. The band at 1450.47 cm^{-1} may be attributed to the aromatic $\nu(\text{C=C})$ stretching vibration. At 1111.00 cm^{-1} , the band is highly intense $\nu(\text{C-O})$ and is related to the $\nu(\text{C-O})$ stretching vibration of the bonds in ester, ether or phenol groups. The band corresponding to 802.39 cm^{-1} in the fingerprint area indicates a mono substituted aromatic structure. The weak absorption band at 678.94 cm^{-1} corresponds to the $\nu(\text{O-H})$ vibration in the benzene ring. The band at 462.92 and 594.08 cm^{-1} which were associated with the in-plane and out-of-plane aromatic ring deformation vibrations common that is quite common for activated carbon.

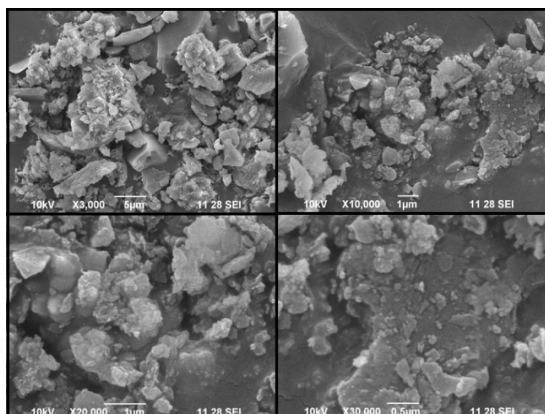


Fig.2. SEM image of Areca Husk Carbon

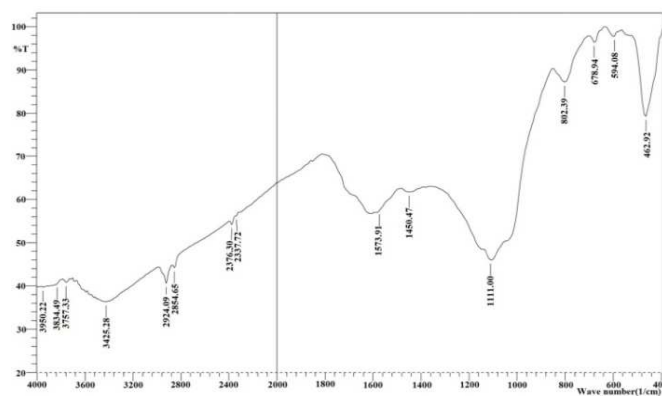


Fig.3. FTIR spectra of AHC

The factorial design

The high and low levels defined for the 2^3 factorial designs were listed in Table 1. The low and high levels for the factors were selected according to some preliminary experiments [6]. The factorial design matrix and % removal was measured in each factorial experiment is shown in Table 1, with the low (-1) and high (+1) levels as specified in Table 1. Percentage removal was determined as average of three parallel experiments. The order in which the experiments were made was randomized to avoid systematic errors. The main effects and interactions between factors were determined [7]. Fig. 4 and 5 illustrates the mean of the experimental results for the respective low and high levels of, pH, Particle Size and temperature. The results were analyzed and along with the main effects the interactions of different factors were determined. The coded mathematical model for 2^3 factorial designs can be given as

$$\%R = X_0 + X_1A + X_2B + X_3C + X_4AB + X_5BC + X_6AC + X_7ABC \quad (2)$$

Where % R is the percentage removal of MG, X_0 is the global mean, X_i represents the other regression coefficients and A, B, C stands for pH, Particle Size and temperature respectively.

Table 1 Factors and levels used in the factorial design

Factor Coded	Symbol	Low Level (-1)	High Level (+1)
pH	A	4	9
Particle Size	B	100	250
T(K)	C	300	320

Analysis of variance (ANOVA)

After estimating the main effects, the interacting factors affecting the removal of MG were determined by performing the analysis of variance (ANOVA). Sum of squares (SS) of each factor quantifies its importance in the process and as the value of the SS increases the significance of the corresponding factor in the undergoing process also increases (Table 2). The main and interaction effects of each factor having P values <0.05 are considered as potentially significant[8].

Table 2 Design matrix and the results of the 2³ factorial design

Trial No.	Coded values of independent variables			% Removal		
	pH	Particle Size	T(K)	Observed	Predicted	Residual
1	1	1	1	76.85	77.14	0.29
2	1	1	1	78.57	78.64	0.07
3	1	-1	-1	79.21	79.63	0.42
4	-1	-1	1	85.31	85.07	-0.24
5	1	-1	-1	86.42	86.06	-0.36
6	-1	1	-1	86.97	86.72	-0.25
7	-1	-1	1	92.80	92.88	0.08
8	-1	1	-1	93.61	93.65	0.04

Main and interaction effects

The effect of each factor was statistically significant at $P < 0.05$ for AHC [9], the main effects A, B and C and interactions AC and BC are of higher statistical significance. Based on F-ratio and P-value statistically insignificant factors were discarded. Fig. 4 and 5 shows the main effects of the process parameters for the AHC onto MG. The sign of the main effect indicates the directions of the effect. It can be seen from Fig.4 the effect of AC, BC and ABC was characterized by a greater degree of departure and also had a negative effect on the response, whereas the effect of A, B, C and AB the concentration positive effect on the response with greater departure. The significant interactions of MG onto AHC were shown in Fig.5. The interaction plots for MG onto AHC showed that interaction of temperature played major role and also temperature factors interacted strongly with other factors indicating predominant influence in removal. After discarding insignificant terms, the resultant models can be represented as:

$$\%R = 86.03 + 0.85*A + 0.41*B + 7.03*C + 0.07*AB - 0.50*BC - 0.21*AC - 0.03*ABC \quad (3)$$

Table 3 Estimated Effects and Coefficients for % Removal (coded units)

Term	Effect	Coefficient	SE Coefficient	T	P
Constant		86.0362	0.04982	1726.85	0.000
PH	1.6957	0.8479	0.06042	14.03	0.000
Particle Size	0.8138	0.4069	0.05939	6.85	0.000
T(K)	14.0661	7.0330	0.06102	115.26	0.000
pH*Particle Size	0.1330	0.0665	0.07202	0.92	0.367
pH*T(K)	-0.9939	-0.4969	0.07400	-6.72	0.000
Particle Size*T(K)	-0.4093	-0.2047	0.07274	-2.81	0.011
pH*Particle Size*T(K)	-0.0630	-0.0315	0.08821	-0.36	0.725
S = 0.2557		PRESS = 2.8990			
R-Sq = 99.86%		R-Sq(pred) = 99.68%		R-Sq(adj) = 99.81%	

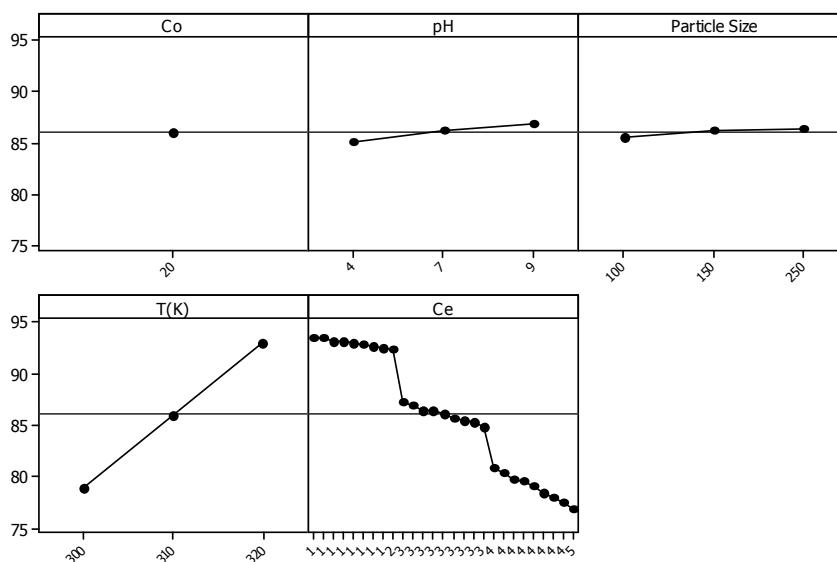


Fig.4. Main effects plot for % removal

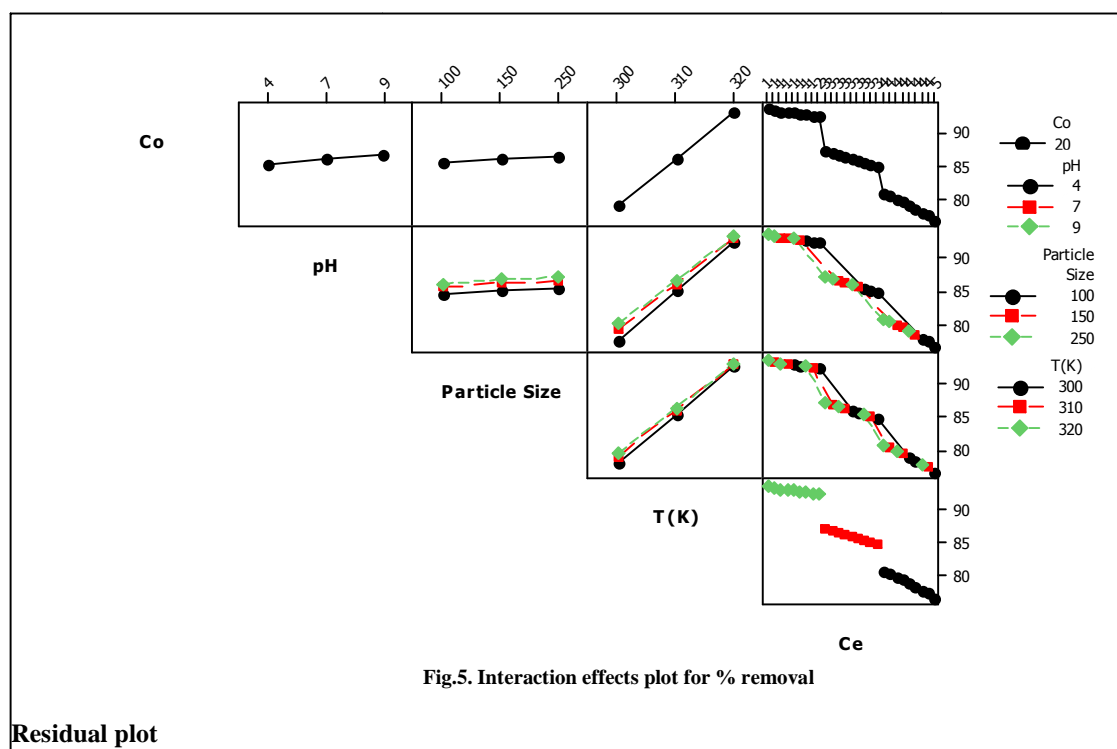


Fig.5. Interaction effects plot for % removal

Residual plot

In fig. 6a shows the assumption of normality of error terms. In this case we see that most of the points are clustered around blue line indication that the error terms are approximately normal. Thus our assumption of normality is valid. In fig. 6b the error terms against the fitted values. There are approximately half of them are above and half are below the zero line indicating that our assumption of error terms having mean zero is valid. On the same graph we see the clear cyclic pattern among the error terms indicating that they are violating the assumption of independence of error. Error terms are not independent. The fig.6d again re-emphasizes the normality assumption. The sample size is just 26

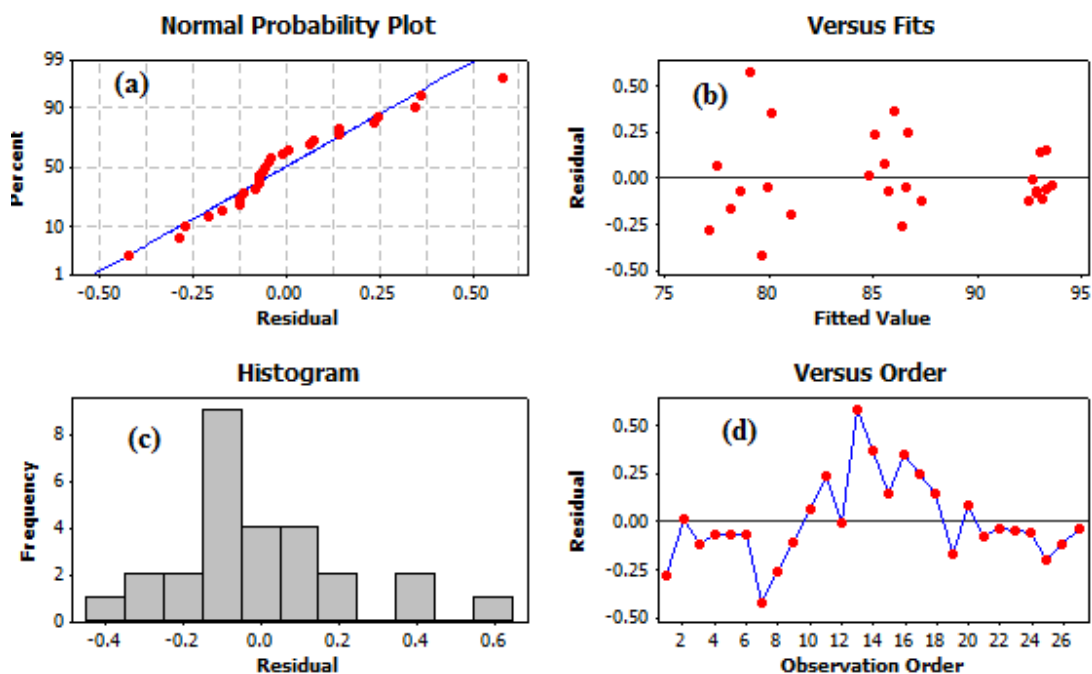


Fig.6. Residual plot for % removal

The Pareto chart

The relative importance of the main effects and their interactions was also observed on the Pareto chart (Fig. 7). The t-test was performed to determine whether the calculated effects were significantly different from zero, these values for each effect was shown in the Pareto chart by horizontal columns [10]. For the 95% confidence level and sixteen degrees of freedom, the t-value is 2.1. As shown in Fig. 7, some values are positioned around a reference line, but these values are not significant factors. The values that exceed a reference line, i.e., those corresponding to the 95% confidence interval, are significant values [11]. According to Fig. 7, the main factors (A, B, and C) and their interactions (AC, and BC) that extend beyond the reference line were significant at the level of 0.05.

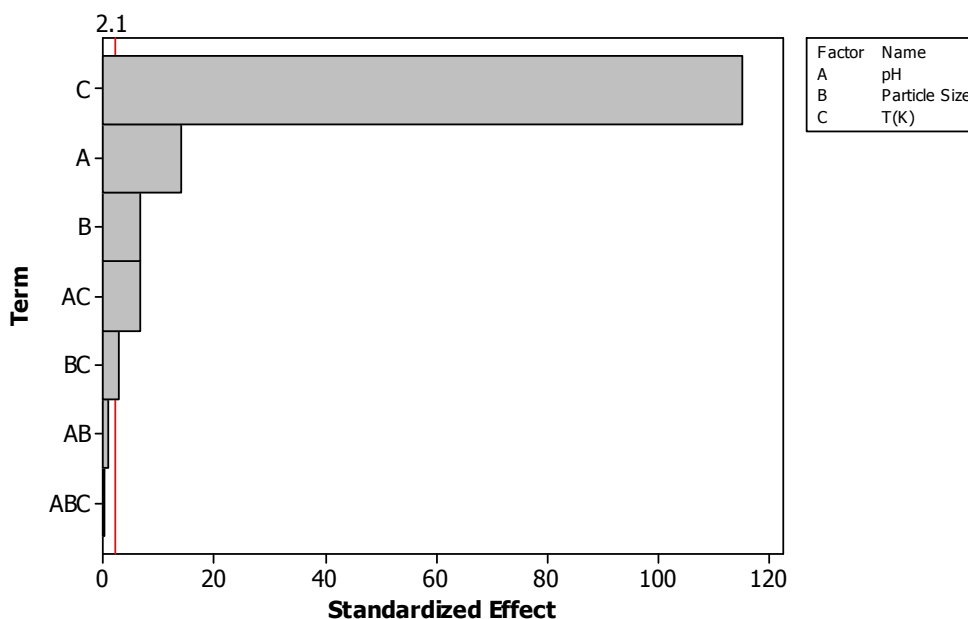


Fig.7. Pareto chart of the standardized effects

The temperature represented the most significant effect on % removal. The pH (A), temperature (C) and interaction (BC & AC) had greater effects on % removal. While, except for the interaction effect between AB and ABC have smaller effects and were statistically significant at 95% confidence.

Normal probability plots

It is not clear whether these results are real or chance. To identify the real effects, a normal probability plot is used. One point on the plot is assigned to each effect. According to the normal probability plots, the points which are close to a line fitted to the middle group of points represent those estimated factors that do not demonstrate any significant affect on the response variables. Points far away from the line likely represent the “real” factor effects [12]. The normal probability plot was given in Fig. 8. The main factors (A, B, and C) and their interactions (AC, and BC) are away from the straight line and are therefore considered to be “real”. Because AC and BC lie to the left of the line, their contribution had a negative effect, A, B and C on the right had a positive effect. The temperature (C) had largest effect because its point lies farthest from the line. These results confirm the previous Pareto chart analysis and the values of Table 3. The second important factor is pH (BC), which was more significant than B (particle size). The effects decreased as $C > A > B > AC > BC > AB > ABC$.

The calculated data from the model (predicted values)[9]. The normal probability plot of residuals for %removal (Fig.8) showed how closely the set of observed values followed the theoretical distribution. Generally, experimental points are reasonably aligned, suggesting a normal distribution. The selected model adequately described the observed data, explaining approximately 99.86% (due to $R^2=0.9986$) of the variability of % removal.

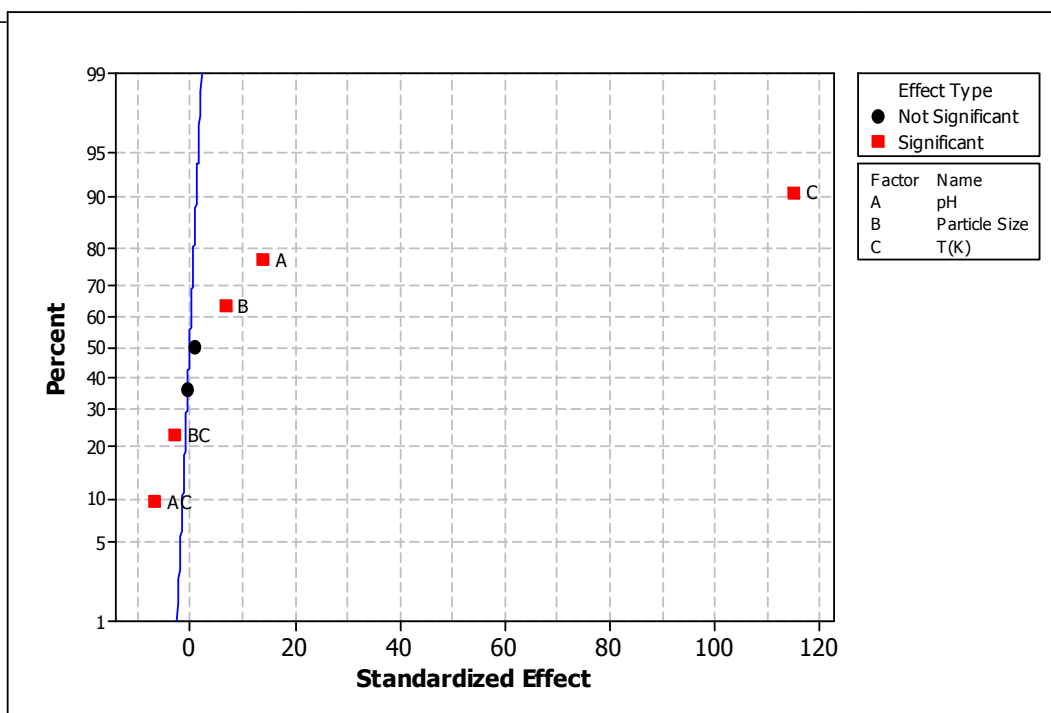


Fig.8. Normal probability plot of standardized effects

Table 4 Analysis of Variance for % Removal (coded units)

Source	DF	Seq SS	Adj SS	Adj MS	F	P
Main Effects	3	903.816	885.094	295.031	4510.12	0.000
2-Way Interactions	3	3.548	3.551	1.184	18.09	0.000
3-Way Interactions	1	0.008	0.008	0.008	0.13	0.725
Residual Error	19	1.243	1.243	0.065		
Total	26	908.615				

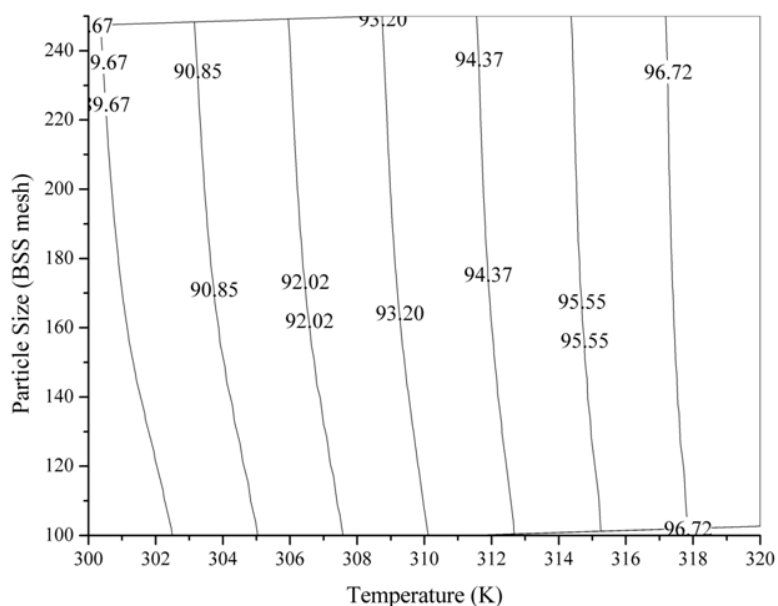


Fig.9. Response contour plot of MG removal (%) showing interactive effect of Temperature and Particle Size

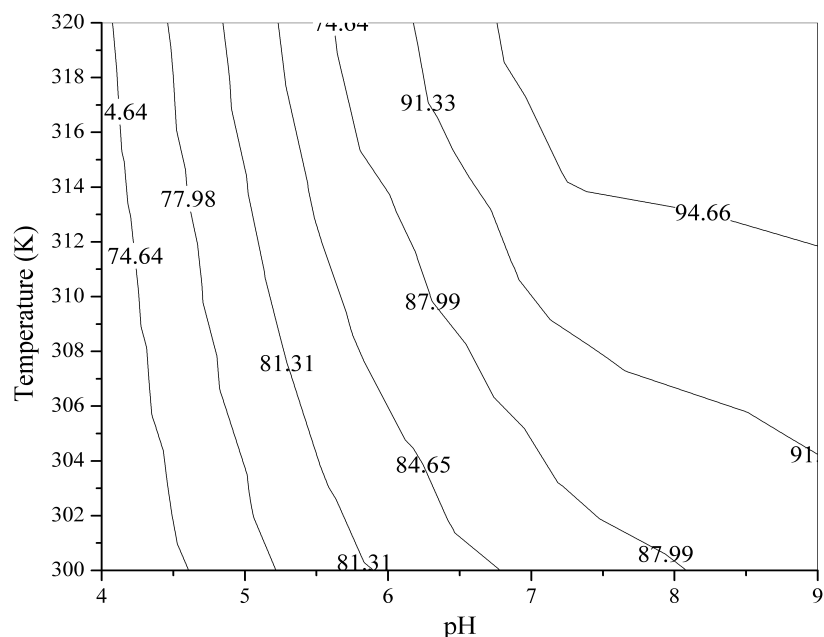


Fig.10. Response contour plot of MG removal (%) showing interactive effect of pH and Temperature

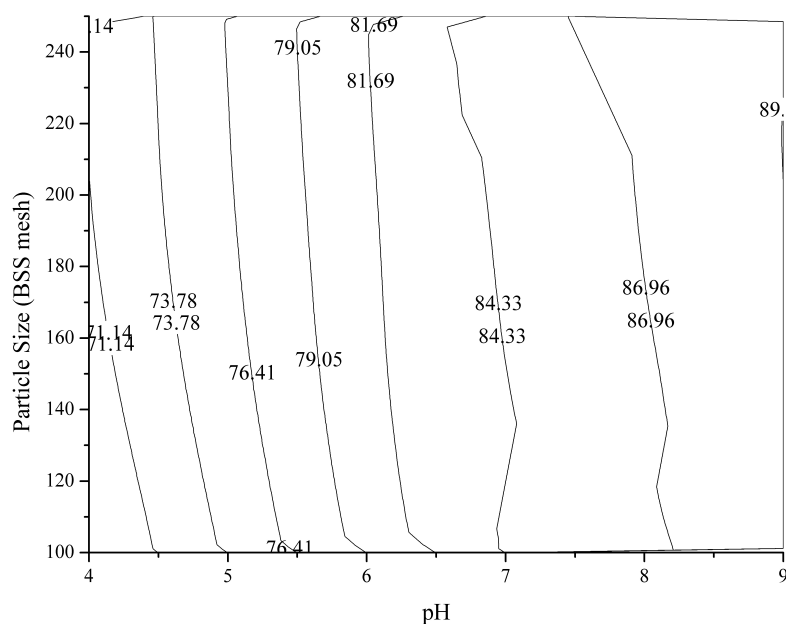


Fig.11. Response contour plot of MG removal (%) showing interactive effect of pH and Particle Size

Contour Plot

The response of contour plot was analyzed and plots were obtained to assess the response of each factor graphically. The response of certain factors is function that describes how the response moves as the level of those factor changes, when the other factors are fixed at their optimum levels. From the Fig.(9-11), it can be observed that each of the three variables used in the present study has its individual response on adsorption. From the contour plots, it has been found that there is a gradual increase in adsorption of dyes with increase in temperature from the lower level 300K (Coded value -1) to the higher level 320K (Coded value +1). Similarly, the adsorption increases with respect to the particle size of AHC from 100 to 250 BSS mesh numbers (Coded value -1 to +1). It is also revealed that the MG dye would have small change to adsorption with respect to pH change. The pH level selected for this study

was 4, 7 and 9 (coded value -1 to +1). The results obtained by adapting factorial design in the study of absorption of various dyes on AHC proves; Process temperature has an adverse effect on the response for AHC. Other parameters like particle size and pH affected the process of adsorption significantly. The experimental values and the predicted values of Factorial design model are in close agreement with quadratic regression >99%.

CONCLUSION

The statistical design of the experiments combined with was applied in optimizing the conditions of maximum adsorption of the dye onto AHC. The optimized conditions of pH, Particle size and Temperature with fixed initial concentration of 20 mg L⁻¹ for MG dye adsorption were found as 9, 250 BSS mesh and 320 K, respectively which correspond to 93.6% adsorption. Temperature was the greatest influence on the amounts of dye removal. The factorial design demonstrated significant interaction between pH and temperature. This interaction had more influence on dye removal than did the other interactions (Temperature-Particle size, pH-Particle size). pH, Particle size and temperature had a negative influence on dye removal, is the validity of this study was limited to pH between 4 -9, particle size 100-250 BSS mesh and temperatures between 300 - 320 K.

Acknowledgements

The authors are grateful to Kumaraguru college of Technology for doing the research by providing some of the equipments for the research

REFERENCES

- [1] GS Gupta; G Prasad; VN Singh, *Water Res.*, **1990**, 24(1), 45-50.
- [2] M Neamtu; A Yediler; I Siminiceanu; M Macoveanu; A Kellrup, *Dyes and Pigm.*, **2004**, 60(1), 61-68.
- [3] RK Wahi; WW Yu; YP Liu; ML Meija; JC Falkner; W Nolte; VL Colvin, *J. Molecular Catal. A: Chem.*, **2005**, 242(1-2), 48-56.
- [4] Mounir Bennajaha; Yassine Darmaneb; Mohammed Ebn Touhamic; Mostapha Maalmia; *Int.J. Engg. Sci. Tech*, **2010**, 2(12), 42-52.
- [5] G McKay; HS Blair; JR Gardner, *J. Appl. Polym. Sci.*, **1982**, 27(8), 3043-3057.
- [6] B Ucar; A Guvenc; U Mehmetoglu, *Hydrol Current Res.*, **2011**, 2(2), 1-8.
- [7] D Kavak, *J. Hazard. Mater.*, **2009**, 163(1), 308-314.
- [8] K Adinarayana; P Ellaiah; B Srinivasulu; R Bhavani Devi; G Adinarayana, *Process Biochemistry*, 38(11), **2003**, 1565-1572.
- [9] NT Abdel Ghani; AK Hegazy; GA El Chaghaby; EC Lima, *Desalination*, 249(1), **2009**, 343-347.
- [10] V Ponnusami; V Krithika; R Madhuram; SN Srivastava, *J. Hazard. Mater.* 142(1-2), **2007**, 397-403.
- [11] T Mathialagan; T Viraraghavan, *Environ. Technol.* 26(5), **2005**, 571-579.
- [12] K Palanikumar; JP Dawim, *J. Mater. Process. Technol.* 209(1), **2009**, 511-519.